ACS OMEGA

http://pubs.acs.org/journal/acsodf

Article

Novel Graphene Wool Gas Adsorbent for Volatile and Semivolatile Organic Compounds

Genna-Leigh Geldenhuys, Yvonne Mason, George C. Dragan, Ralf Zimmermann, and Patricia Forbes*

Cite This: *ACS Omega* 2021, 6, 24765−24776

Read Online

ACCESS | Metrics & More | Article Recommendations | Supporting Information

ABSTRACT: Volatile and semivolatile organic compounds in ambient air and occupational settings are of great concern due to their associated adverse human health and environmental impacts. Novel graphene wool samplers have been developed and tested to overcome limitations of commercially available sorbents that can only be used once and typically require solvent extraction. Graphene wool (GW) was synthesized by non-catalytic chemical vapor deposition with optimized conditions, resulting in a novel fibrous graphene wool that is very easy to manage and less rigid than other forms of graphene, lending itself to a wide range of potential applications. Here, the air pollutant sampling capabilities of the GW were of interest. The optimal packing weight of GW inside a glass tube (length 178 mm, i.d. 4 mm, o.d. 6 mm) was investigated by the adsorption of vaporized alkane standards on the GW, using a condensation aerosol generator in a temperature-controlled chamber and subsequent detection using a flame ionization detector. The optimized GW packing density was found to be 0.19 mg mm^{-3} at a flow rate of 500 mL min^{-1}, which provided a gas collection efficiency of >90% for octane, decane, and hexadecane. The humidity uptake of the sampler is less than 1% (m/m) for ambient humidities <70%. Breakthrough studies showed the favorable adsorption of polar molecules, which is attributed to the defective nature of the graphene and the inhomogeneous coating of the graphene layers on the quartz wool, suggesting that the polar versus non-polar uptake potential of the GW can be tuned by varying the graphene layering on the quartz wool substrate during synthesis. Oxidized domains at the irregular edges of the graphene layers, due to a broken, non-pristine sp^2 carbon network, allow for adsorption of polar molecules. The GW was applied and used in a combustion sampling campaign where the samplers proved to be comparable to frequently used polydimethylsiloxane sorbents in terms of sampling and thermal desorption of non-polar semivolatile organic compounds. The total alkane concentrations detected after thermal desorption of GW and PDMS samplers were found to be 17.96 ± 13.27 and 18.30 ± 16.42 $\mu g\ m^{-3}$, respectively; thus, the difference in the alkane sampling concentration between the two sorbent systems was negligible. GW provides a new, exciting possibility for the monitoring of organic air pollutants with numerous advantages, including high sampling efficiencies, simple and cost-effective synthesis of the thermally stable GW, solvent-free and environmentally friendly analysis, and, importantly, the reusability of samplers.

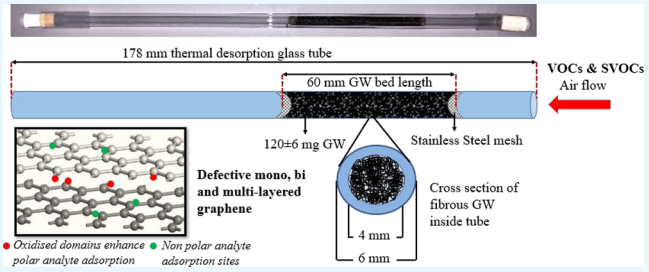

1. INTRODUCTION

Air quality is of global concern, and efficient means to monitor air pollutants is critical, particularly those which require monitoring by law due to the environmental and human health impacts they may incur. Volatile and semivolatile organic compounds (VOCs and SVOCs, respectively) are emitted to the atmosphere from numerous sources, such as the petrochemical, agricultural, paint, and mining industries. Current commercially available carbon-based sorbents, including activated charcoal, Anasorb 747, Carboxen, and carbon molecular sieves, used to sample VOCs and SVOCs in air typically require solvent extraction prior to analysis, which is costly, time-consuming, and environmentally unfriendly, and they cannot be reused, which increases operational costs.

Graphene is a crystalline allotrope of carbon nanomaterials that has received worldwide attention due to its unique two-dimensional planar monolayer structure, outstanding chemical and thermal stability, high specific surface area, and hydrophobic properties which deem graphene to be a suitable sorbent candidate.[1−6] The recognition of graphene's properties resulted in a number of potential applications in electronics, energy storage, catalysis, and gas sorption, storage, separation, and sensing.[2,7−10] The majority of graphene materials in environmental applications see their use in sensing and storage; however, to the best of our knowledge, graphene has not been used as a sorbent material for organic gas-phase pollutants for environmental sampling to date. The aim of our research was to develop a novel graphene wool (GW) trap and

Received: July 8, 2021
Published: September 13, 2021

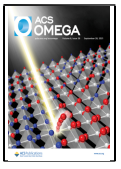

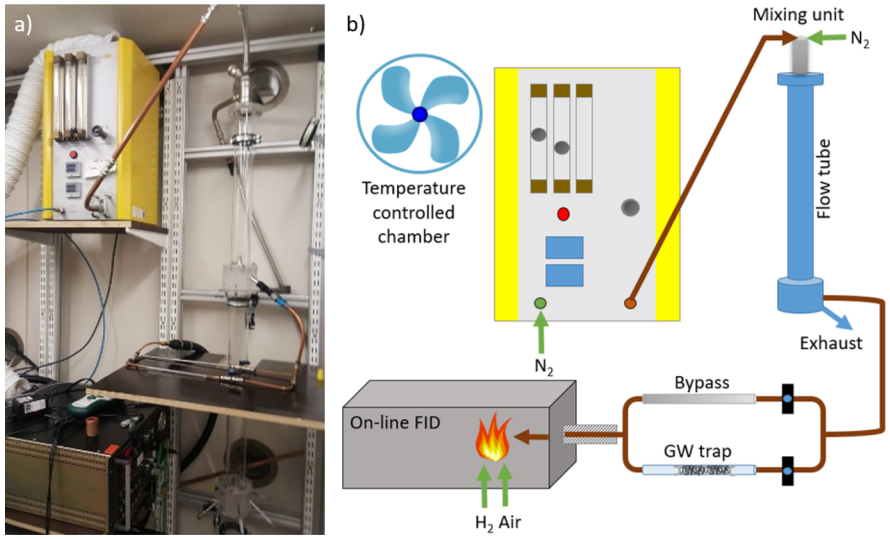

Figure 1. Experimental setup for the determination of gas collection efficiency on the GW trap (a) and schematic of the experimental setup (b).

evaluate its application as a sorbent material for ambient and occupational air pollution sampling of SVOCs and VOCs.[11,12]

The GW trap samplers which we have developed can be thermally desorbed for analysis (which does not use solvents and is thus more environmentally friendly and cost-effective), and importantly, they can be conditioned and reused multiple times. The low back pressure of the GW sampler also enables the use of a small portable battery-operated personal sampling pump, whereby the GW trap can be used as a standalone sorbent or in a sampling train with other sampling media. In this paper, the GW adsorbents were evaluated in terms of gas-phase collection efficiencies, breakthrough volumes, and humidity uptake. Following this, their real-life application was demonstrated in a fuel emission sampling campaign.

2. MATERIALS AND METHODS

2.1. Chemicals and Synthesis of GW. Commercially available 9−30 μm coarse quartz wool (Arcos Organics, New Jersey, USA) was used as a substrate for the growth of graphene by atmospheric pressure chemical vapor deposition (APCVD), as reported in Schoonraad.[13] The quartz wool was placed in the center of a horizontal quartz tube (50 mm o.d., 44 mm i.d., × 1000 mm length) of a OTF 1200X-50-5L high-temperature furnace (MTI Corporation, California, USA). A 500:500 sccm argon (99.999%, Afrox, South Africa): hydrogen (99.999%, Afrox, South Africa) mix was introduced into the system after which the temperature was ramped to 1200 °C. After a 10 min annealing period, 100 sccm methane (99.95%, Afrox, South Africa) was introduced for 30 min for graphene growth. The system was rapidly cooled under Ar and H_2 after the growth period had elapsed. The deposited graphitic carbon takes the form of the quartz wool substrate by covering the surface of each fiber, and for the purpose of its application, the substrate was not removed; thus, the term "graphene wool (GW)" in this work infers graphene coated on quartz wool. The synthesis steps, optimization, and full characterization of GW (Raman spectroscopy, scanning electron microscopy (SEM), high-resolution X-ray photoelectron spectroscopy (XPS), and high-resolution transmission electron microscopy (TEM)) are detailed in Schoonraad et al.[12,13]

2.2. Assembly and Optimization of the GW Trap. To assemble the final, optimized GW traps (Figure S1), 120 ± 6 mg of synthesized GW was weighed out using a calibrated Sartorius Entris analytical balance. The GW was gently packed into 178 mm-long glass tubes (i.d. 4 mm, o.d. 6 mm, Listco, SA) using tweezers and an in-house manufactured wire tool consisting of a 10 cm straight wire (o.d 2 mm) with one side bent into a hook. The GW was packed into a bed length of 50 mm and was held securely in place using stainless-steel screens (Merck, SA). The GW samplers were conditioned for 8 h at 300 °C with hydrogen (≥99.999% purity, AFROX, SA) with a gas flow of 100 mL min^{-1} using a Gerstel TC 2 tube conditioner (Chemetrix, SA). The open ends of the conditioned traps were then capped with endcaps consisting of 1 cm quartz glass rods secured with Teflon sleeves.

In order to determine the final parameters of the GW trap (120 g of GW packed into 50 mm bed length), the assembly of the GW trap was first optimized by determining the maximum gas-phase collection efficiency with varying masses (50, 99, 110, and 120 mg) of the sorbent material at different bed lengths (20, 35, 50, and 55 mm) using the experimental setup as described in Section 2.3.

2.3. Gas-Phase Collection Efficiency of the GW Trap. The substance-specific gas-phase collection efficiency of the GW trap was investigated using vaporized octane (C8), dodecane (C12) (99%, Merck, Hohenbrunn, Germany), and hexadecane (C16) (99%, Alfa Aesar, Karlsruhe, Germany) in an experimental setup as depicted in Figure 1, which was a similar setup used by Kohlmeier et al. who validated multichannel silicone rubber traps as denuders for gas−particle partitioning of aerosols from semivolatile organic compounds.[14] Each substance was individually vaporized using a Sinclair-La-Mer 270 condensation aerosol generator at flow rates of 2.5 L min^{-1} for octane and 5 L min^{-1} for dodecane and hexadecane, followed by dilution with nitrogen to a total flow of 50 L min^{-1}. The generated vapor was then passed through a 150 cm-long flow tube to ensure that the generated vapor was below the saturation concentration of each substance and avoid droplet formation. The resultant gas was redirected through either a bypass line or a GW trap via copper tubing. The alternate switching between the bypass line and the graphene trap was made possible using two-way valves, and the subsequent concentration of gas molecules was measured with a 109A-type flame ionization detector (FID) (J. U. M.

https://doi.org/10.1021/acsomega.1c03595
ACS Omega 2021, 6, 24765−24776

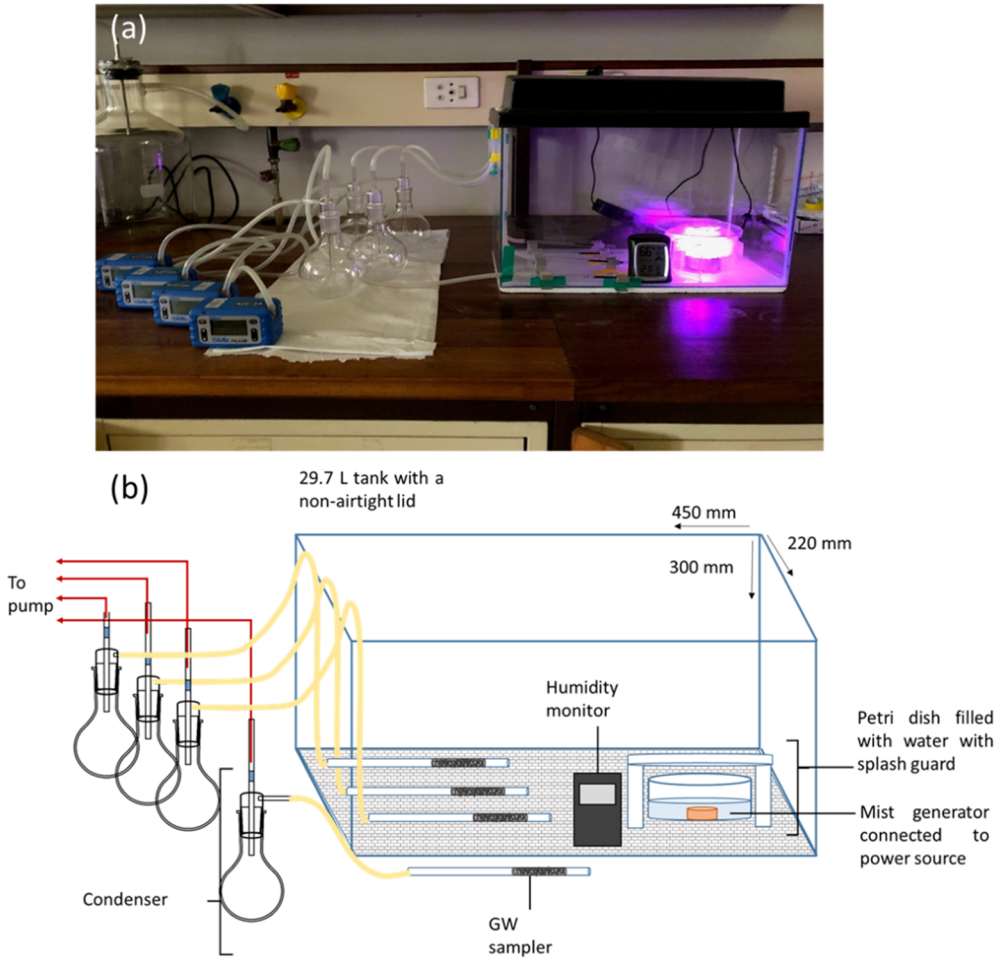

Figure 2. Experimental setup for the determination of humidity uptake on GW traps (a) and schematic of the experimental setup (b).

Engineering, Karlsfeld, Germany), which was operated at a flow rate of 0.5 L min^{-1}. The FID was calibrated daily with propane (Linde, Germany), and the instrument zero was validated using pure nitrogen (Linde, Germany). The concentration ratio measured between the GW trap and bypass line was used to obtain the time-dependent gas-phase collection efficiency (%) as in eq 1

$$\text{Collection efficiency} = \left(1 - \left(\frac{C_{\text{Trap}}}{C_{\text{Bypass}}}\right)\right) \times 100 \quad (1)$$

To ensure that the detected concentration was not biased from the adsorption of gases onto the copper tubing surface, the lines were saturated prior to the experiment by inserting an empty liner in place of the GW trap and verifying a constant FID signal. All experiments were performed in triplicate inside a temperature-controlled chamber at 24.7 ± 0.2 °C.

Three different GW traps were used in each experiment, and the traps were conditioned with nitrogen gas (Linde, Germany) for 5 h at 230 °C in between subsequent experiments to successfully demonstrate the reusability and reproducibility of the novel adsorbent. In order to determine the strength of adsorption and thus storage capabilities of GW, nitrogen gas was passed through a loaded trap to check if any FID signal was observed, which would indicate that the analytes were desorbing from the GW and breakthrough had occurred.

2.3.1. Comparative Traps Used in Gas Collection Efficiency Experiments. The PDMS samplers were prepared based on the method described by Ortner and Rohwer.[15] Each trap consisted of 22 parallel PDMS tubes, with a total mass of 385 mg, (55 mm long, 0.3 mm i.d., 0.6 mm o.d., Sil-Tec, Technical Products, Georgia, US) in a 178 mm-long glass tube (6 mm o.d., 4 mm i.d., Listco, SA). The PDMS traps were conditioned prior to use at 280 °C for 16 h using hydrogen (≥99.999% purity, AFROX, SA) with a gas flow of 100 mL min^{-1} using a Gerstel TC 2 tube conditioner. The PDMS samplers were capped identically to the GW traps in Section 2.2. Commercially available activated charcoal adsorbent tubes (Drager, type BIA, Lübeck, Germany) were also used to compare gas-phase collection efficiencies of VOCs.

2.4. Moisture Uptake by the GW. The humidity uptake on GW traps was tested gravimetrically using the setup illustrated Figure 2. A fish tank (450 mm × 220 mm × 300 mm, Lifestyle Pet Hyper, SA) was used as the humidity chamber, and an aquarium mist maker (M-12L, Sobo, China), submerged in water inside a Petri-dish (110 mm i.d., 115 mm o.d., 64 mm height), was used to generate aerosols that simulated set ambient humidity ranges >75%. A makeshift splash guard was placed above the Petri-dish to allow only a fine mist to flow from the dish and to prevent larger water droplets from splashing out and compromising the study. Aluminum stands held the samplers in place at the same height as the ambient air humidity monitor (Monitor de la Humedad,

https://doi.org/10.1021/acsomega.1c03595
ACS Omega 2021, 6, 24765−24776

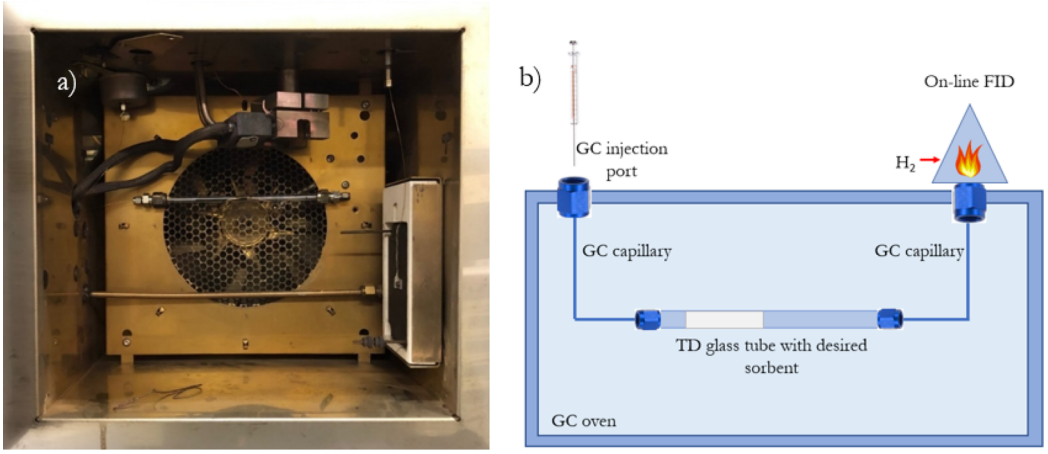

Figure 3. Experimental setup within the GC oven for the determination of breakthrough volume (a) and schematic of the experimental setup (b).

AcuRite, US). Teflon tubing was used to connect the samplers to Gilian GilAir Plus air sampling pumps (Sensidyne, US) via a condenser to prevent water from entering the pumps. GW samplers were conditioned, using a Gerstel TC 2 tube conditioner (Chemetrix, SA), with H_2 at 250 °C for 5 h prior to use and were weighed before and after the hygroscopicity experiment to determine the gross uptake of humidity by mass on the GW traps.

Triplicate GW samplers were placed inside the chamber to sample the air for a period of 10 min at a flow rate of 500 mL min^{-1} at three set humidities (50, 60, and 70%). The mist generator was switched off, and the lid was removed during this study to obtain a constant humidity with no undesired variations due to air flow effects. A GW sampler was also connected outside the chamber as a control, which was sampled in parallel to other samples. For humidity ranges >75%, the mist generator was switched on, and the lid was placed on the tank to simulate a more humid environment than what was typically experienced under ambient conditions. A GW trap was then compared to a quartz wool (QW) control trap for humidity ranges >75% to accurately assess the effect the graphene layers have on the moisture uptake. The entrained moisture was investigated by weighing the GW trap after sampling and then flicking the trap 10 times consecutively and reweighing the trap in order to determine how much of the moisture was absorbed versus that physically entrained in the fibers of the sorbent.

2.5. Experimental Determination of Breakthrough Volumes. Breakthrough volumes as a function of temperature were determined using the setup depicted in Figure 3. An uncoated capillary column (15 cm, 0.25 mm i.d., 0.363 mm d.f., SGE Analytical Science) was connected to each end of the GW trap using relevant nuts and ferrules with one of the uncoated capillaries connected directly to the injection port of a Varian 6890 gas chromatograph (GC) (Agilent, US), and the second capillary connected the other end of the GW trap to a FID such that the GW trap took the place of the GC column. The inlet pressure of the GC injection port was held at 8 kPa, and H_2 was used as the carrier gas at a flow rate of 10 mL min^{-1}. The FID H_2 gas flow was set at 40 mL min^{-1} with the air and N_2 make-up flow rates at 400 and 10 mL min^{-1}, respectively. N_2 was generated using a Peak Scientific nitrogen generator (Peak Scientific, Scotland), while hydrogen, dry air, and helium (≥99.999% purity) were supplied by AFROX (SA). Once the sampler was connected to the uncoated capillaries and was securely positioned in the GC oven, the setup was leak-tested using a gas leak detector (LD-223, GL Sciences Inc., Japan).

The chosen sorbents to which the breakthrough volumes of the GW sampler were compared were the PDMS trap as it has historically been used in a wide range of air-monitoring studies and a sampler made of quartz wool to the same specifications of the GW sampler as a control. The GC oven was operated isothermally at set temperatures for each experimental run, which was done in duplicate; thereafter, the temperature was increased in suitable increments until a satisfactory Gaussian peak was observed on the FID chromatogram. The set temperatures were between 25 and 190 °C, 25 and 200 °C, and 25 and 340 °C for the GW, QW, and PDMS samplers, respectively.

The breakthrough volume for the samplers was calculated using the retention times from the experimentally acquired FID chromatograms for the GW, PDMS, and QW samplers using eq 2.[16] As this research aimed to develop a new sampler, the mass of the sorbent to be used in the sampler was not fixed, as this aspect was to be optimized; therefore, BV is reported in units of volume per g of sorbent

$$\mathrm{BV} = \frac{(\mathrm{RT} \times \mathrm{flow})}{W_a \times 1000\ \mathrm{mL/L}} \tag{2}$$

where BV = breakthrough volume (L g^{-1}), RT = retention time of the analyte (min), flow = carrier gas flow (mL min^{-1}), W_a = specific sorbent mass (g), and 1000 mL/L = conversion factor to convert data from mL g^{-1} to L g^{-1}.

In the case of the QW, GW, and PDMS, these masses were found to be 0.141, 0.120, and 0.366 g, respectively.

The FID chromatograms were produced by injecting 1 μL of each of the following nine analytes into the GC injection port—methanol (bp 64.7 °C), hexane (bp 68 °C), propanol-2-ol (82.5 °C), toluene (bp 110.6 °C), butan-1-ol (bp 117.7 °C), octane (bp 125.6 °C), cyclohexanone (bp 155.6 °C), dodecane (216.2 °C), and hexadecane (286.8 °C). These analytes were chosen due to their range of boiling points and their differing polarities in order to investigate the effect that both parameters have on the interaction between an analyte and the selected sorbents. Methanol (≥99% purity) and *n*-hexane (≥97% purity) were purchased from Sigma-Aldrich (SA). Propanol-2 (≥99% purity), butan-1-ol, (≥99% purity), and dodecane (≥99% purity) were purchased from Merck. Cyclohexanone

https://doi.org/10.1021/acsomega.1c03595
ACS Omega 2021, 6, 24765−24776

(≥98.5% purity) was purchased from UNILAB (Philippines); octane (≥99.5% purity) and hexadecane (≥99.5% purity) were purchased from BDH laboratory reagents (SA). Acetone (≥97% purity) and toluene (≥99.5% purity) were obtained from Associated Chemical Enterprises (ACE, SA).

The temperature increments of the breakthrough experiments differed as the temperature increments were dependent on the sorbent and the tested analyte. A minimum of four temperature increments were used. The duplicate chromatographic FID data for each sampler were then averaged for each analyte at the specific isothermal temperature run, and the retention time of the selected analyte for the point corresponding to where the maximum signal occurred was taken from the averaged results. Thereafter, eq 2 was used to calculate the temperature-dependent breakthrough volume for a range of VOCs on GW, PDMS, and QW.

2.6. Application of the GW Sampler. *2.6.1. CAST Experimental Setup.* A combustion aerosol standard (CAST, Jing mini-CAST 5201D, Switzerland) generator was operated with propane (99.95%, Linde AG, Germany) according to settings described by Mason et al.[17] Rapeseed oil methyl ester (RME) fuel was one of the fuels tested and was purchased from ASG Analytik-Service GmbH, Augsburg, Germany. The fuel was introduced to the CAST generator using a high-performance liquid chromatography (HPLC) pump (Kontron, type 420, Germany), which generated 22 L min^{-1} undiluted combustion exhaust, which then passed through a series of online analytical instrumentation (a FID (SK-Electronik, GMBH) and a Fourier transform infrared spectroscopy (FT-IR) gas analyzer (Gasmet, Model: DX4000, Finland)). After online analysis, 0.3 L min^{-1} undiluted CAST exhaust was introduced to a porous tube dilutor (Mikro-Glasfaser Filter-element, Type GF-12-57-80E) to which dry air was added to make up a total diluted flow of 3 L min^{-1}. An ejector dilutor drew 3 L min^{-1} from the porous dilutor and diluted the flow with synthetic air at 27 mL min^{-1}, after which a custom-built three-way Y-piece stainless-steel splitter was fitted to allow for the diluted flow to be directed to selected samplers, which included PDMS and GW traps that sampled at a flow rate of 500 mL min^{-1} for 10 min with GilAir Plus air-sampling pumps. A full description of the CAST setup is described by Mason et al., where this system was used to sample gas-phase volatile and semivolatile organic fuel emissions from three different fuels.[17]

2.6.2. GC−MS Analysis. Samplers were thermally desorbed using helium at 60 mL min^{-1} from 80 °C to 250 and 280 °C for PDMS and GW samplers, respectively, with a hold time of 30 min using a thermal desorption system (TD-20, Shimadzu, Japan). The cooled injection system (CIS) method was ramped from 5 to 330 °C and held for 30 min. For analysis, a GC-2010 Plus was coupled to a MS-QP2010 Ultra (both Shimadzu, Japan), and the helium carrier gas was set at a flow rate of 1.6 mL min^{-1} with a split ratio of 10:1 using a VF-XMS 30 m × 0.25 mm i.d. × 0.25 μm d.f. column (Agilent, Netherlands). The GC oven was initially held at 60 °C for 6 min and then ramped at 5 °C min^{-1} to 250 °C. The transfer line temperature was set to 250 °C. The mass spectrometry method scanned mass ranges of m/z 35−500 with an electron ionization energy of 70 eV and an ion source temperature of 230 °C. Calibration of the GW and PDMS was performed using individually prepared standards of alkanes in hexane (2−200 ng μL^{-1} made from alkane standard solution C_8−C_{20}, Sigma-Aldrich, Supelco, US) that were spiked onto traps with 1 μL of internal standard mix (*n*-heptane d_{16}, *n*-dodecane d_{26}, and *n*-hexadecane d_{34}, Sigma-Aldrich, Supelco, US). The concentrations of the internal standards can be found in Table S1.

3. RESULTS AND DISCUSSION

3.1. Optimization of the GW Trap Assembly in Terms of GW Mass, Volume, and Density. In order to determine the final parameters of the GW trap, the assembly of the GW trap was first optimized by determining the maximum gas-phase collection efficiency at varying masses of the sorbent material at different bed lengths, resulting in varying densities that are depicted in Table 1.

Table 1. Density, Mass, and Volume of GW Packed Into a Glass Tube for the Optimization Study

mass of GW (mg)	bed length (mm)	volume of GW (mm^3)	density of GW packing (mg mm^{-3})
50	70	879.645	0.0568
50	35	439.823	0.1137
50	20	251.327	0.1989
99	50	628.318	0.1576
110	55	691.150	0.1592
120	50	628.318	0.1910

In order to achieve the optimal packing of the sorbent material in a glass tube, where the tube dimensions were chosen to be compatible with a commercial thermal desorber, the gas-phase collection efficiency for octane was investigated at varying masses of the GW sorbent material. The gas-phase collection efficiency of the GW was then compared to that of two other gas-phase samplers—a PDMS trap and a commercially available activated charcoal adsorbent tube. Figure 4a reveals that the GW gas-phase collection efficiency increased from 42 to 94% when increasing the GW mass from 0.01 to 0.11 g in the glass tube, which was then comparable to the collection efficiency of activated charcoal. However, it must be noted that the GW mass in the trap was significantly less than the mass of charcoal required to achieve the same results. The charcoal has the advantage of excellent VOC adsorption but the tradeoff is more difficult desorption that requires time-consuming solvent extraction steps. The activated charcoal has a mass of 900 mg in a bed length of 69 mm, and due to its high surface area and high degree of microporosity, the gas molecules penetrate deep into the sorbent pores when compared to the GW, which is only a thin surface layer of graphene, as seen in TEM images of the material in Schoonraad et al., which is why thermal desorption is possible with GW and not charcoal.[12]

The PDMS absorbent (with a mass of 365 mg) proved to be an ineffective medium for the collection of volatile organic species, such as octane, as the premature fall in the FID signal quickly increased to 50% of the bypass signal within a few seconds, indicating that breakthrough from the trap was occurring, and gas-phase collection efficiency was just above 40%. This was not a surprising finding, considering the fact that PDMS has been validated for trapping of SVOCs.[18−20] This can be explained by the mechanism and kinetics, which are entirely different for PDMS in that absorption of analytes takes place instead of adsorption as in the case of charcoal and GW.

Another important practical aspect favoring the use of GW is the sampling back pressure (BP). The BP is the resistance

https://doi.org/10.1021/acsomega.1c03595
ACS Omega 2021, 6, 24765−24776

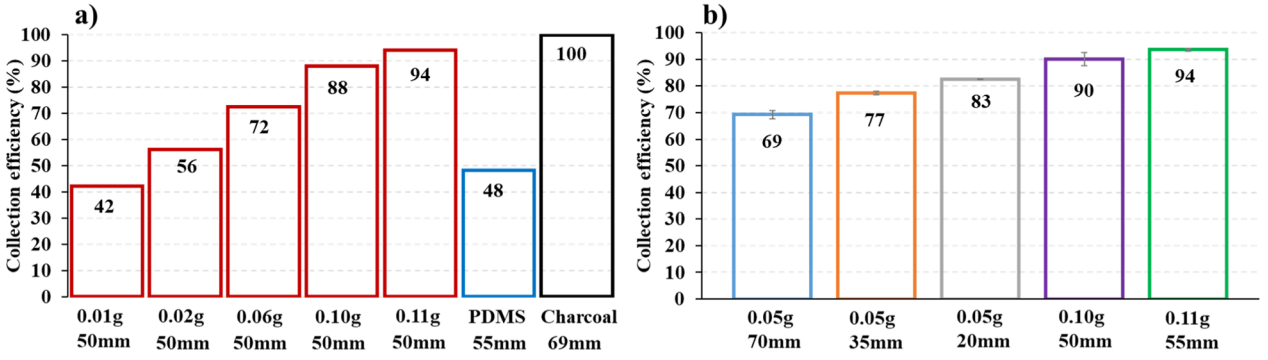

Figure 4. (a) Octane collection efficiency of GW traps as a function of increasing mass of GW but constant bed length, in comparison to PDMS and charcoal traps and (b) octane collection efficiency of GW traps as a function of packing density which was varied by altering the bed length (mm) of the GW inside the glass tube with the error bars showing standard deviation for $n = 3$.

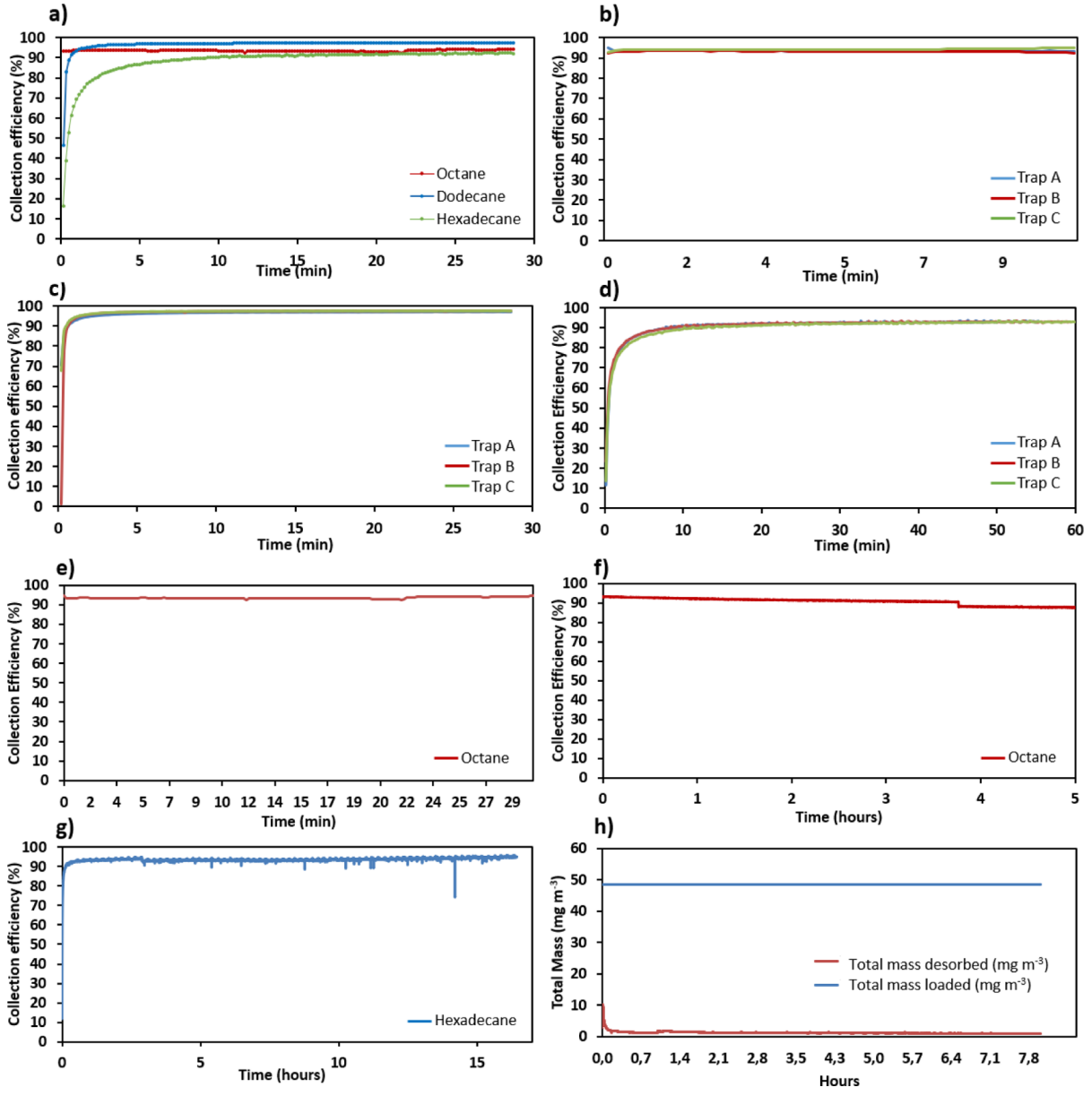

Figure 5. Average gas collection efficiency of C8, C12, and C16 alkanes on GW traps A−C (a). Individual collection efficiency of octane (b), dodecane (c), and hexadecane (d) on three different GW traps. Desorption of octane over a period of 30 min (e) and 5 h (f) and of hexadecane over 15 h (g). The total concentration desorbed versus the total concentration loaded of dodecane on the GW trap over a period of 8 h (h).

https://doi.org/10.1021/acsomega.1c03595
ACS Omega 2021, 6, 24765−24776

Table 2. Moisture Uptake of GW Traps at Various Levels of Humidity (n = 3)

average humidity	average mass of the GW sampler before exp (g)	average mass of the GW sampler after exp (g)[a]	average mass difference (g)	% (m/m) H_2O on trap
50%[b]	6.3488	6.3489	0.0001	0.0817
60%	6.3604 ± 0.0096	6.3607 ± 0.0094	0.0003 ± 0.0005	0.2180 ± 0.3775
70%	6.3612 ± 0.0100	6.3616 ± 0.0099	0.0004 ± 0.0001	0.3321 ± 0.0861
extreme	6.3646 ± 0.0183	6.4272 ± 0.0047	0.0626 ± 0.0147	51.9439 ± 12.6622

[a]Mass recorded after removing entrained moisture. [b]Based on one GW trap, as no mass difference was found for the other two traps.

opposing the desired air flow through the sampler that may lead to unstable sampling flow rates at high BPs. The BP of the GW traps was found to be ±13″ H_2O at a constant flow of 400 mL·min^{-1}, as measured and displayed using the GilAir portable sampling pumps. The low back pressure can be attributed to the low sorbent packing density of the GW and its fibrous nature, which adds to the versatility of samplers as it allows them to be used with a personal sampling pump (BP threshold of 40″ H_2O) in a variety of sampling setups, including denuders.[20]

The effect of the packing density of the GW trap was investigated by keeping the mass of the GW constant and varying the bed length. From Figure 4b, it is evident that the gas-phase collection efficiency is inversely proportional to the bed length, which is due to the mean free path of the analyte decreasing with a more compact bed, resulting in higher rates of gas collection. When maintaining a GW mass of 50 mg, the gas collection efficiency increased from 69 to 77% when decreasing the bed length by a factor of 2 and further improved to an average of 83% when the bed length was decreased to 20 mm. The GW mass was then doubled to improve the capacity of the GW trap further. Taking all the assembly parameters in this study into consideration, the optimal GW trap assembly consisted of 120 ± 20 mg of GW housed in a glass tube (5.0 mm o.d. × 4.0 mm i.d.) with a 50 mm bed length corresponding to a density of 0.19 mg mm^{-3}. The collection efficiency of the octane was also determined to be 94 ± 0.5% for three different GW traps with the same packing density, which confirms repeatability of the experiments and reproducibility of the manmade trap assembly.

3.2. Gas Collection Efficiency of GW Traps. Three replicate traps (A−C) were made according to the optimized assembly as set out in Section 3.1 and were then used to determine the gas collection efficiency with three different alkanes ranging from the more volatile octane to the semivolatile hexadecane. Figure 5a shows the average collection efficiency of octane (C8), dodecane (C12), and hexadecane (C16) on three different GW traps A−C, and Figure 5b−d shows the individual gas-phase collection efficiencies for octane, dodecane, and hexadecane, respectively. The collection efficiency was very good at over 90% for all three alkanes over a period of 30 min. When switching from the bypass line, it can be clearly seen that the time taken to reach the maximum collection efficiency was significantly longer for hexadecane due to the slower adsorption kinetics;[14] similarly, dodecane adsorption on the GW was slower than that of octane; this follows Fick's Law of diffusion, which is governed by the molecule size-dependent diffusion coefficient. The vapor pressure also leads to differences in the vapor saturation concentration of the tested substances, and since octane has the highest vapor pressure, saturation is reached faster due to the higher number of molecules available to be adsorbed on the lines, which can only adsorb a finite number of molecules.

In order to determine the strength of adsorption and thus storage capabilities of GW, nitrogen gas was passed through a loaded trap to check if any FID signal was observed, which would indicate that the analytes were desorbing from the GW and breakthrough was occurring. Figure 5e reveals that the octane collection efficiency remained unchanged after a period of 30 min, but after a period of 4 h, a breakthrough of <5% was observed in Figure 5f. To confirm this finding, the experiment was repeated with the less-volatile hexadecane over an extended period of 15 h, and no significant breakthrough occurred (Figure 5g). This experiment will also be beneficial for the future investigation of displacement mechanisms if mixtures of gas-phase analytes are to be sampled. The breakthrough experiment of dodecane, illustrated in Figure 5h, showed that <2% of the total adsorbed concentration of 48.42 mg m^{-3} was desorbed after a period of 8 h.

The affinity of graphene for alkanes has been demonstrated theoretically,[21] and it was found that the desorption energy increases as a function of the n-alkane chain length, which supported our experimental data as we found hexadecane to have the highest affinity for the GW. When optimizing the atomic positions during adsorption, the authors found that all calculations reached an energetic minimum when the alkane carbon skeletons were parallel to the graphene surface.[21] However, the GW in this study is not pristine graphene, so it is likely that the adsorption of gas molecules on the defective GW is much stronger, and the orientation of the adsorbates may differ.[10]

This work proves the excellent affinity and capacity of the GW for non-polar analytes in the volatile and semivolatile ranges. These GW traps can also be used for extended periods of time without breakthrough, which renders them as potentially suitable samplers for full 8 h-shift occupational monitoring.

3.3. Humidity Study. Molecular adsorbates can act as either acceptor or donor molecules when interacting with graphene, and H_2O has been found to be an acceptor adsorbate, resulting in p-type doping of the graphene, whereby the water molecules adsorb only on the surface of the graphene, as the hydroxyl groups are too large to penetrate the graphene film.[10,22−24]

As mentioned previously, a high sample humidity can have an influence on the type and extent of molecular adsorption of other analytes on the GW, and it can lead to a decrease in their breakthrough volume as a result of reduced availability of active sites on the GW surface; thus, hygroscopicity studies are vital to determine the feasibility of a novel sorbent. Table 2 represents the moisture uptake of GW traps as a function of humidity.

Samples were taken in triplicate in different humidity ranges from 50 to 70%, which are commonly experienced in ambient

https://doi.org/10.1021/acsomega.1c03595
ACS Omega 2021, 6, 24765−24776

and occupational environments. Samples were also taken in triplicate inside the controlled-humidity chamber under visibly humid conditions where extremely high-humidity environments were artificially produced using a mist generator. This experiment was conducted to investigate the extent of the H_2O adsorption on the GW surface versus water droplets that are entrained within the GW fiber layers and cavities in the trap. After sampling, the GW sampler was weighed and compared to the dry-conditioned trap to reveal that the mass of the sorbent had doubled, representing over 100% moisture uptake. After flicking the trap 10 times consecutively and reweighing the trap, it was found that over 40% of the moisture was not physically adsorbed. Based on this finding, the entrained moisture was removed from all traps after sampling in the same fashion. The specific mass of GW in each trap was used to calculate % (m/m) H_2O for each replicate (GW in sampler 1: 0.1223500 g, GW in sampler 2: 0.1198255 g, and GW in sampler 3: 0.1198255 g).

The results in Table 2 show that moisture uptake in the GW traps increased with increasing humidity with values of 0.08, 0.22, and 0.33% (m/m) H_2O for average humidity levels of 50, 60, and 70%, respectively. The moisture uptake is considered insignificant at these humidities, but caution must be taken at higher humidity where the H_2O molecules will compete with analyte molecules for active sites on the GW surface. It is recommended that the GW sampler is not to be used in extremely high-humidity environments unless coupled with an upstream moisture trap.

The interaction between water adsorbates and the graphene surface is largely dictated by the orientation of the water molecules with respect to the surface of the graphene and the structure of the graphene surface itself, whether it is defective, doped, or pristine.[10] This was confirmed by Leenaerts et al., who used density functional theory (DFT) to demonstrate that the adsorption energy was primarily determined by the orientation of the molecule and to a lesser extent by the molecule position.[25] In our study, the defective SiO_2 substrate promotes adsorption from water molecules, as the defects in the GW result in oxygen-containing species at the surface, as confirmed by XPS,[12] which interact with the polar water molecules. It was even found that H_2O adsorbates can shift the SiO_2 substrate's impurity bands and change their hybridization with the graphene bands.[26] This is in contrast to pristine graphene that is non-polar in nature and thus more insensitive to H_2O adsorbates with the only mechanism of adsorption being physisorption by weaker dispersive forces.[22,25,26]

3.4. Chromatographic Determination of the Breakthrough Volume of Selected Analytes. Breakthrough analysis is expedient to determine the maximum loading capacity of the sorbent before breakthrough and/or loss of the analyte occurs, which in turn will be used to determine suitable sampling volumes. The adsorption and desorption of analytes on the GW surface were investigated by breakthrough analysis at room temperature and at elevated temperatures.

In Section 3.2, the excellent gas collection of non-polar, planar alkanes in the volatile and semivolatile ranges was demonstrated; therefore, this section will extend to the more polar and volatile range. Here, the elution technique was utilized, whereby the Gaussian gas chromatographic peaks depicted in Figure 6 for each VOC and SVOC were used in conjunction with eq 2[16] to determine the specific breakthrough volume. It should be noted that the methodology used is based on the literature; however, the injection of pure liquid samples

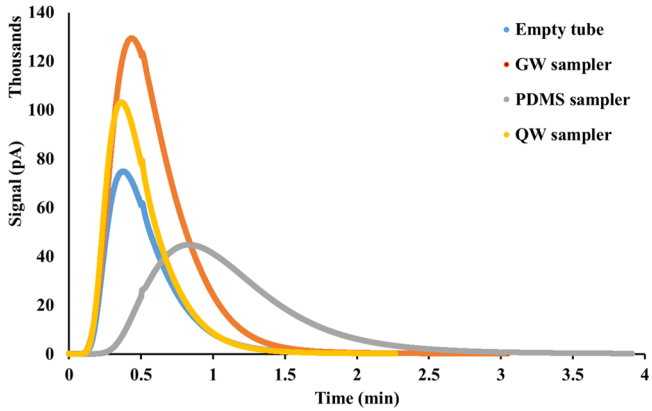

Figure 6. Overlaid chromatograms illustrating the differing retention of methanol at 25 °C for samplers used in the breakthrough study.

may lead to overloading of the sorbents. The results should thus be seen as providing comparative measurements between sorbents but may not reflect the true gas-phase breakthrough volumes. The average retention times used for the calculations at isothermal temperatures for each sorbent are reported in Tables S2–S4. The dead volume correction was not done, as this value required the injection of a non-retained analyte into the GC port, and typical non-retained analytes, such as methane, have been found to be adsorbed by graphene.[6]

The resultant breakthrough curves for each analyte on each sampler type are represented in Figure 7, and their corresponding exponential equations and correlation coefficients are shown in Table S6. The exponential equations derived from the curves were used to calculate the BV values for analytes, which could not be measured experimentally, due to retention by sorbents at this temperature, and these values are presented in Table 3. From the curves in Figure 7, it is immediately evident that all BVs decrease with increasing temperature, and GW showed significantly higher breakthrough volumes for polar analytes when compared to PDMS samplers.

The studied polar VOCs were selected to represent a range of boiling points from 64.7 to 155.6 °C. The correlation coefficients (R^2 values in Table S5) ranged from 0.7570 to 0.9902, which shows a good fit to experimental data, enabling extrapolation to 25 °C in order to determine the breakthrough volumes at ambient sampling temperatures. Calculated GW BVs predictably increased with decreasing volatility of the analyte, but the low BVs obtained, ranging from 0.029 to 0.202 L g^{-1}, demonstrated that in this experiment, non-polar VOCs did not have a very strong affinity for the GW surface. Other sorbent materials such as Tenax have specific breakthrough volumes (SBVs), an order of magnitude larger than for GW, but it must be noted that the polarity of this sorbent lends itself to polar adsorbates.

From Figure 7 and Table 3, it can be seen that at room temperature (25 °C), the GW breakthrough volume for the most volatile compound, methanol, is calculated to be 0.058 L g^{-1}. However, when targeting analytes with higher boiling points such as cyclohexanone, the breakthrough volume is calculated to be 0.563 L g^{-1}. When considering a more semivolatile, non-polar compound such as hexadecane, the BV decreases to 0.202 L g^{-1}.

The extrapolated breakthrough volume at a specific temperature should be considered when selecting the sampling

https://doi.org/10.1021/acsomega.1c03595
ACS Omega 2021, 6, 24765−24776

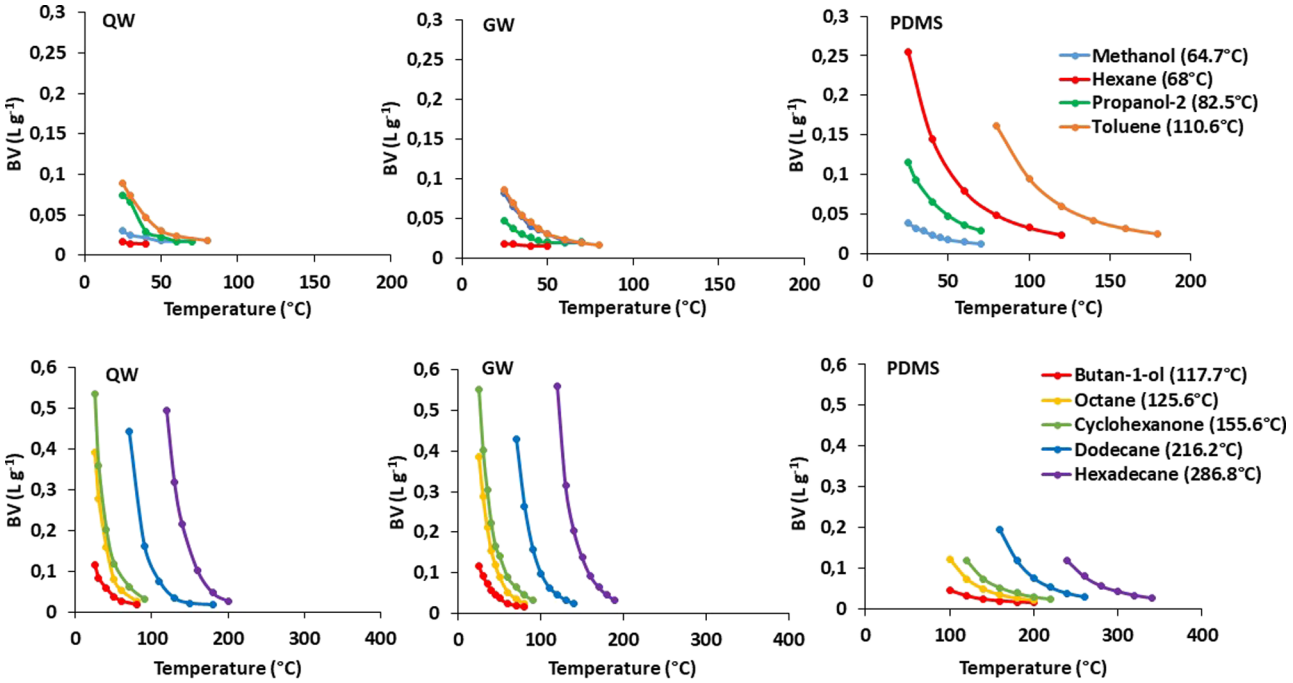

Figure 7. Breakthrough volume curves for the 0.120 g QW (left), 0.141 g GW (middle), and 0.365 g PDMS (right) samplers at various isothermal temperatures.

Table 3. BVs of QW, GW, and PDMS along with the Boiling Points, Molecular Masses, and Densities of the Compounds at the Inlet Temperature of 250 °C[27]

analyte with the corresponding BP	polarity expressed as Log *P*	MM of compounds (g mol^{-1})	density at 25 °C (g L^{-1})	QW BV at 25 °C (L g^{-1})	GW BV at 25 °C (L g^{-1})	PDMS BV at 25 °C (L g^{-1})
			Polar Compounds			
methanol (64.7 °C)	−0.77	32.04	0.875	0.043	0.058	0.044
propanol-2 (82.5 °C)	0.05	60.10	0.79	0.086	0.093	0.120
butan-1-ol (117.7 °C)	0.88	74.12	0.81	0.405	0.397	0.168[a]
cyclohexanone (155.6 °C)	0.81	98.15	0.94	0.549	0.563	0.227[a]
			Non-polar Compounds			
hexane (68 °C)	3.90	86.18	0.66	0.029	0.029	0.259
toluene (110.6 °C)	2.73	92.14	0.86	0.102	0.097	0.185[a]
octane (125.6 °C)	5.18	114.23	0.70	0.128	0.129	0.194[a]
dodecane (216.2 °C)	6.10	170.33	0.75	0.170[a]	0.142[a]	0.266[a]
hexadecane (286.8 °C)	8.30	226.41	0.77	0.212[a]	0.202[a]	0.347[a]

[a]Calculated values are distinguished from the experimentally determined values.

flow rate and sample volume and additional parameters such as sampling humidity, which also influences the breakthrough behavior of an analyte due to the adsorbed water molecules taking up active adsorption sites on the surface of the GW, which was discussed in Section 3.3.

From Table 3, it can be seen that PDMS has larger breakthrough volumes for all non-polar analytes, whereas GW showed higher breakthrough volumes for all polar analytes.

To establish the extent of adsorption of the GW surface, the BV volumes were directly compared to those of the parent QW substrate. GW shows higher BV at 25 °C than QW for almost every analyte; however, these differences are not considered significant. This can be explained by the non-uniform bi- and multilayered graphene surface on the QW. Regions of the QW are exposed on the GW, resulting in the same adsorption mechanisms of polar analytes and therefore similar retention and breakthrough. These findings suggest that the growth of graphene on the QW could be further optimized in terms of the surface coverage and level of defects to enhance molecular interactions with both polar and non-polar analyte molecules.

When comparing the GW sorbent to the PDMS sorbent, which has already been validated for PAHs and more polar compounds,[14,20] it can be seen from Table 3 and Figure 7 that GW had higher BVs for methanol, butan-1-ol, dodecane, and cyclohexadecane. The PDMS, on the other hand, showed better BVs for non-polar analytes only, which can be explained by the differences in the sorbent material. The PDMS is a non-polar medium that traps analytes by absorption rather than adsorption; therefore, only molecules with the same polarity will be absorbed. The GW sorbent showed an increase in BVs with an increase in the carbon chain length of the non-polar analytes, which was also seen in the gas collection efficiency study in Section 3.2, and it can be rationalized by the increase in desorption energy, as determined theoretically by Londero and colleagues.[21] The affinity of the GW for polar molecules is due to the defective nature of the GW that contains polar

https://doi.org/10.1021/acsomega.1c03595
ACS Omega 2021, 6, 24765−24776

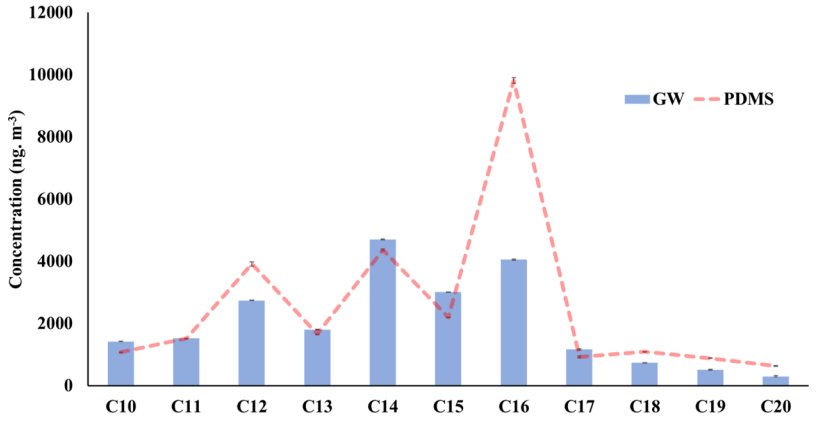

Figure 8. Concentration of C_{10}−C_{20} alkanes in RME biodiesel combustion emissions on GW and PDMS samplers that were thermally desorbed and analyzed by GC−MS.

regions with increased electrostatic potential and increased dispersive forces for polar analyte adsorption. Oxidized domains exist in the material as a result of a broken sp^2 carbon network, which occurred during CVD synthesis.[13] These domains occur at the irregular edges of the graphene layers and are the main site of adsorption of polar molecules due to interactions with electronegative oxygen, resulting in dispersive forces, of which hydrogen bonding is the most predominant. A similar result was reported by Berashevich and Chakraborty, who found that adsorbed polar molecules formed a cluster along the oxidized zigzag edges of graphene. The oxidized edges tend to donate a charge to the adsorbates, and the extent of adsorption is governed by the intermolecular distance and by the location of the adsorbed molecules relative to the plane of graphene.[28]

The BV for octane, dodecane, and hexadecane in this study was significantly lower than that determined in the gas collection efficiency study in Section 3.2, and it must be noted that the experimental setups were different, which plays a major role in the results obtained, specifically when the temperature is concerned. The temperature-controlled chamber was held at ambient temperature during all measurements, whereas this FID experimental setup had a heated inlet, resulting in an increase in the kinetic energy of analytes, leading to an increased rate of desorption and thus lower BVs. Another drawback of this study was that only one GW trap was used in the configuration, as it was not practicably feasible to change the sampler after each experiment. This can result in a deterioration of the GW coating with time and an increase in defects, which ultimately affect the polarity and retention capabilities of the sampler; therefore, the results must be interpreted with caution. It is suggested that further investigation is required in order to accurately determine the GW material interaction with polar versus non-polar analytes. In this study, the peak areas for methanol on GW were found to be significantly higher than for other samplers (Figure 6), and it was hypothesized that the graphene material is broken down when it is flushed with certain solvents, such as methanol, which resulted in the elevated FID signal in the experiment. This is another aspect to the novel material that requires further research in order to fully understand the uses and limitations of the sampler.

For future work in this regard, it is advised to further optimize the GW sampler to contain a higher mass of the GW sorbent per sampler to increase the BVs and then introduce a second GW sampler downstream to potentially act as a gauge for breakthrough. This will allow for more accurate determination of the SBVs for target analytes under varying conditions, which are encountered in real-world sampling. Headspace gas sampling should be conducted where the breakthrough of analytes can be determined by means of permeation tubes, as in the experiments conducted here, overloading of the sorbents was likely resulting under non-linear chromatographic conditions. A good starting point would be the determination of breakthrough of naphthalene using headspace sampling, as this can directly be compared to the validation of PDMS sorbents, for which the breakthrough volume of naphthalene is 5 L at a sampling flow rate of 0.500 L min^{-1}.[29]

3.5. Application of the GW Sampler in Fuel Combustion Emission Sampling. The GW sampler and various other samplers were used in conjunction with a controlled-combustion aerosol standard system, where duplicate air combustion emission measurements were taken from diesel, gas-to-liquid fuel, and rapeseed methyl ester biofuel, as described in detail by Mason et al.[17] For the scope of this study, only one fuel, namely, RME biodiesel, was considered to demonstrate the practical use of the GW sampler.

From Figure S1, it can be clearly seen that the GW calibration curves for C_{10}−C_{20} alkanes had correlation coefficients >0.999 for every analyte, which depicts excellent linearity for the range of concentrations with LODs ranging from 424 to 4874 ng m^{-3}, as seen in Table S6 in the Supporting Information. The linear response also demonstrated the successful thermal desorption of analytes from the GW, therefore showing that no solvent extraction is required. The fact that TD quantitatively removes the non-polar C_{10}−C_{20} alkane analytes, with molecular weights and boiling points ranging from 114 to 282 g mol^{-1} and 125.6 to 343 °C, respectively, from the sampler further confirms the sustainable reusability of the samplers with respect to these analytes.

The GW sampler was shown to be very effective in sampling alkanes in the volatile−semivolatile range, which were found to be in the low μg m^{-3} range with tetradecane being the most abundant, as seen in Figure 8. The performance of the GW sampler was directly compared to that of a PDMS sampler, which has been tested, validated, and applied in numerous studies,[14,17−20,30,31] and it was found to be very comparable in both emission profiles and concentrations of each analyte, excluding hexadecane, with an % difference of 1.9% between

https://doi.org/10.1021/acsomega.1c03595
ACS Omega 2021, 6, 24765−24776

the total alkane concentrations. The GW showed higher recoveries of the lower alkanes <C15 when compared to the PDMS but lower concentrations for the higher alkanes. The significantly large discrepancy between the two samplers for hexadecane (83% difference) and all alkanes >C15 was likely due to incomplete thermal desorption of heavier alkanes from the GW, as the TD method was optimized for PDMS. These findings were consistent with those found in Section 3.2, which demonstrated the high affinity of GW for non-polar analytes, but were contrary to those found in Section 3.4, which showed better retention of polar analytes on the GW. This can be explained by better coverage of graphene layers on the QW for the traps used in the CAST study and the fact that each GW sampler was only used once, ensuring the integrity of the graphene surface.

4. CONCLUSIONS

A novel GW trap was optimized in terms of sorbent mass, bed length, and packing density and was tested for use as a sampler for a range of volatile and semivolatile analytes. The GW sampler was compared to commercially available and validated PDMS and charcoal samplers to assess accuracy and efficacy. The gas-phase collection efficiency was found to be >94% for octane, dodecane, and hexadecane at ambient temperatures, which was comparable to that of activated charcoal. The humidity uptake onto GW was found to be insignificant where moisture was predominantly found to be entrained in the fibers and not physisorbed on the graphene surface. The experimental and theoretical breakthrough studies showed that GW had higher breakthrough volumes for polar analytes when compared to the PDMS sampler, however BVs of GW did not significantly increase when compared to QW, which demonstrated the high degree of defects of the GW and the non-uniform surface of bi- and multilayers. Subsequently, a more practical breakthrough experiment may be required, such as using headspace sampling, to aid in the validation of the retention volumes at set pressures and temperatures using numerous replicates of different GW traps.

The GW sampler efficacy was then demonstrated in a real-world application, where it was employed as an air sampler for volatile and semivolatile organic compounds arising from the combustion of a rapeseed methyl ester biofuel. The linear response of each analyte demonstrated the successful thermal desorption of the C_{10}−C_{20} alkane analytes from the GW sampler, therefore, showing that no solvent extraction is required. The GW was found to be very comparable in both emission profiles and concentrations of each analyte to a PDMS sampler and can be used as a standalone sampler or as a secondary trap in a sampling train similar to that of a PDMS denuder setup.[19,20]

GW is thus a novel adsorbent that has proven to be an effective sampling medium comparable to currently available technologies. It has numerous advantages including the fact that it is reusable, sustainable and cost-effective and, very importantly, does not require time-consuming and toxic solvent extraction techniques. Another significant advantage is the possibility to tune the surface chemistry of the GW for targeted polar or non-polar analytes by modifying the surface coverage of graphene on the QW. The presence of oxidized domains at the edges of the non-pristine graphene results in dispersive forces with polar analytes due to interactions with the electronegative oxygen and results in edge-type adsorption. The extent of polar adsorption is thus largely governed by the intermolecular distance, the extent of oxidation of the graphene, and the location of the adsorbed molecules relative to the graphene layer plane.

This tunability can also provide additional capabilities regarding device design, for applications including filtration, microfluidics, chemical sensing, and, as in this study, chemical sampling.

■ ASSOCIATED CONTENT

Supporting Information

The Supporting Information is available free of charge at https://pubs.acs.org/doi/10.1021/acsomega.1c03595.

The Supporting Information provides a photograph of the optimized graphene wool sampler assembly; internal standards information; additional breakthrough volume data; and limits of detection and quantification and calibration curves for the target analytes which were thermally desorbed from the GW samplers (PDF)

■ AUTHOR INFORMATION

Corresponding Author

Patricia Forbes − *Department of Chemistry, University of Pretoria, Pretoria 0001, South Africa;* orcid.org/0000-0003-3453-9162; Phone: +27 12 420 5426; Email: patricia.forbes@up.ac.za

Authors

Genna-Leigh Geldenhuys − *Department of Chemistry, University of Pretoria, Pretoria 0001, South Africa; Processing Laboratory, Impala Platinum Limited, Rustenburg 0299, South Africa;* Present Address: Skin Rejuvenation Technologies, Irene, Pretoria, 0157, South Africa

Yvonne Mason − *Department of Chemistry, University of Pretoria, Pretoria 0001, South Africa*

George C. Dragan − *Joint Mass Spectrometry Centre, Cooperation Group "Comprehensive Molecular Analytics", Neuherberg D-85758, Germany;* Present Address: Federal Institute for Occupational Safety and Health, D-44149 Dortmund, Germany.

Ralf Zimmermann − *Joint Mass Spectrometry Centre, Cooperation Group "Comprehensive Molecular Analytics", Neuherberg D-85758, Germany; Joint Mass Spectrometry Centre, Institute of Chemistry, University of Rostock, Rostock D-18051, Germany*

Complete contact information is available at: https://pubs.acs.org/10.1021/acsomega.1c03595

Author Contributions

The manuscript was written through contributions of all authors. All authors have given approval to the final version of the manuscript.

Funding

Funding provided by the University of Pretoria, Impala Platinum Ltd. and the National Research Foundation of South Africa (NRF, grant number 105807) is acknowledged. This work was supported by the German Federal Ministry of Education and Research (BMBF), research contract 01DG17023.

Notes

The authors declare no competing financial interest.

■ ACKNOWLEDGMENTS

The National Research Foundation (NRF, grant number 105807) and the Departments of Chemistry and Physics at the University of Pretoria and Impala Platinum Ltd are acknowledged for their support and resources. The Helmholtz Zentrum and Federal Ministry of Education and Research (BMBF) in Germany are also duly acknowledged with special thanks to the Comprehensive Molecular Analytics (CMA) group at Helmholtz Zentrum München.

■ REFERENCES

(1) Zhang, G.; Guo, X.; Wang, S.; Wang, X.; Zhou, Y.; Xu, H. New graphene fiber coating for volatile organic compounds analysis. *J. Chromatogr. B: Anal. Technol. Biomed. Life Sci.* **2014**, *969*, 128−131.
(2) Wang, T.; Huang, D.; Yang, Z.; Xu, S.; He, G.; Li, X.; Hu, N.; Yin, G.; He, D.; Zhang, L. A review on graphene-based gas/vapor sensors with unique properties and potential applications. *Nano-Micro Lett.* **2016**, *8*, 95−119.
(3) Singh, V.; Joung, D.; Zhai, L.; Das, S.; Khondaker, S. I.; Seal, S. Graphene based materials: Past, present and future. *Prog. Mater. Sci.* **2011**, *56*, 1178−1271.
(4) Yousefi, N.; Lu, X.; Elimelech, M.; Tufenkji, N. Environmental performance of graphene-based 3D macrostructures. *Nat. Nanotechnol.* **2019**, *14*, 107−119.
(5) Chen, Z.; Guo, X.; Zhu, L.; Li, L.; Liu, Y.; Zhao, L.; Zhang, W.; Chen, J.; Zhang, Y.; Zhao, Y. Direct growth of graphene on vertically standing glass by a metal-free chemical vapor deposition method. *J. Mater. Sci. Technol.* **2018**, *34*, 1919−1924.
(6) Zhu, Z. W.; Zheng, Q. R. Methane adsorption on the graphene sheets, activated carbon and carbon black. *Appl. Therm. Eng.* **2016**, *108*, 605−613.
(7) Eda, G.; Fanchini, G.; Chhowalla, M. Large-area ultrathin films of reduced graphene oxide as a transparent and flexible electronic material. *Nat. Nanotechnol.* **2008**, *3*, 270−274.
(8) Ramanathan, T.; Abdala, A. A.; Stankovich, S.; Dikin, D. A.; Herrera-Alonso, M.; Piner, R. D.; Adamson, D. H.; Schniepp, H. C.; Chen, X.; Ruoff, R. S.; et al. Functionalized graphene sheets for polymer nanocomposites. *Nat. Nanotechnol.* **2008**, *3*, 327−331.
(9) Xu, S.; Man, B.; Jiang, S.; Yue, W.; Yang, C.; Liu, M.; Chen, C.; Zhang, C. Direct growth of graphene on quartz substrates for label-free detection of adenosine triphosphate. *Nanotechnology* **2014**, *25*, 165702.
(10) Kong, L.; Enders, A.; Rahman, T. S.; Dowben, P. A. Molecular adsorption on graphene. *J. Phys.: Condens. Matter* **2014**, *26*, 443001.
(11) Schoonraad, G.; Forbes, P. B.C. Air Pollutant Trap. SA provisional patent application 2019/00674. 2019. Filed 1 February 2019.
(12) Schoonraad, G.-L.; Madito, M. J.; Manyala, N.; Forbes, P. Synthesis and optimisation of a novel graphene wool material by atmospheric pressure chemical vapour deposition. *J. Mater. Sci.* **2020**, *55*, 545−564.
(13) Schoonraad, G.; Forbes, P. B. C.Graphene wool and manufacture thereof, PCT International Application PCT/ZA2020/050005. Filed 24 January 2020.
(14) Kohlmeier, V.; Dragan, G. C.; Karg, E. W.; Schnelle-Kreis, J.; Breuer, D.; Forbes, P. B. C.; Rohwer, E. R.; Zimmermann, R. Multi-channel silicone rubber traps as denuders for gas-particle partitioning of aerosols from semi-volatile organic compounds. *Environ. Sci.: Processes Impacts.* **2017**, *19*, 676−686.
(15) Ortner, E. K.; Rohwer, E. R. Trace analysis of semi-volatile organic air pollutants using thick film silicone rubber traps with capillary gas chromatography. *J. High Resolut. Chromatogr.* **1996**, *19*, 339−344.
(16) Manura, J. J. Calculation and Use of Breakthrough Volume Data Scientific Instrument Services (SIS): Adaptas Solutions. 2019, [Available from: https://www.sisweb.com/index/referenc/resin10.htm].(accessed on April, 17th 2021).
(17) Mason, Y. C.; Schoonraad, G.-L.; Orasche, J.; Bisig, C.; Jakobi, G.; Zimmermann, R.; Forbes, P. B. C. Comparative sampling of gas phase volatile and semi-volatile organic fuel emissions from a combustion aerosol standard system. *Environ. Technol. Innovation* **2020**, *19*, 100945.
(18) Forbes, P.B.; Rohwer, E.R. Investigations into a novel method for atmospheric polycyclic aromatic hydrocarbon monitoring. *Environ. Pollut.* **2009**, *157*, 2529−2535.
(19) Geldenhuys, G.; Rohwer, E. R.; Naudé, Y.; Forbes, P. B. C. Monitoring of atmospheric gaseous and particulate polycyclic aromatic hydrocarbons in South African platinum mines utilising portable denuder sampling with analysis by thermal desorption-comprehensive gas chromatography-mass spectrometry. *J. Chromatogr. A* **2015**, *1380*, 17−28.
(20) Forbes, P. B. C.; Karg, E. W.; Zimmermann, R.; Rohwer, E. R. The use of multi-channel silicone rubber traps as denuders for polycyclic aromatic hydrocarbons. *Anal. Chim. Acta* **2012**, *730*, 71−79.
(21) Londero, E.; Karlson, E. K.; Landahl, M.; Ostrovskii, D.; Rydberg, J. D.; Schröder, E. Desorption of n-alkanes from graphene: a van der Waals density functional study. *J. Phys.: Condens. Matter* **2012**, *24*, 424212.
(22) Wang, W. L.; Kaxiras, E. Graphene hydrate: theoretical prediction of a new insulating form of graphene. *New J. Phys.* **2010**, *12*, 125012.
(23) Bunch, J. S.; Verbridge, S. S.; Alden, J. S.; Van Der Zande, A. M.; Parpia, J. M.; Craighead, H. G.; McEuen, P. L. Impermeable atomic membranes from graphene sheets. *Nano Lett.* **2008**, *8*, 2458−2462.
(24) Romero, H. E.; Joshi, P.; Gupta, A. K.; Gutierrez, H. R.; Cole, M. W.; Tadigadapa, S. A.; Eklund, P. C. Adsorption of ammonia on graphene. *Nanotechnology* **2009**, *20*, 245501.
(25) Leenaerts, O.; Partoens, B.; Peeters, F. M. Adsorption ofH2O,NH3, CO,NO2, and NO on graphene: A first-principles study. *Phys. Rev. B: Condens. Matter Mater. Phys.* **2008**, *77*, 125416.
(26) Wehling, T. O.; Lichtenstein, A. I.; Katsnelson, M. I. First-principles studies of water adsorption on graphene: The role of the substrate. *Appl. Phys. Lett.* **2008**, *93*, 202110.
(27) PubChem. 2021, [Available from: https://pubchem.ncbi.nlm.nih.gov/]. (accessed on May, 14th 2021).
(28) Berashevich, J.; Chakraborty, T. Doping graphene by adsorption of polar molecules at the oxidized zigzag edges. *Phys. Rev. B: Condens. Matter Mater. Phys.* **2010**, *81*, 205431.
(29) Forbes, P. B. Development of a Laser Induced Fluorescence Technique for the Analysis of Organic Air Pollutants, Doctoral dissertation, University of Pretoria, 2010.
(30) Munyeza, C. F.; Kohlmeier, V.; Dragan, G. C.; Karg, E. W.; Rohwer, E. R.; Zimmermann, R.; Forbes, P. B. C. Characterisation of particle collection and transmission in a polydimethylsiloxane based denuder sampler. *J. Aerosol Sci.* **2019**, *130*, 22−31.
(31) Dragan, G. C.; Kohlmeier, V.; Orasche, J.; Schnelle-Kreis, J.; Forbes, P. B. C.; Breuer, D.; Zimmermann, R. Development of a Personal Aerosol Sampler for Monitoring the Particle-Vapour Fractionation of SVOCs in Workplaces. *Ann. Work Exposures Health* **2020**, *64*, 903−908.

https://doi.org/10.1021/acsomega.1c03595
ACS Omega 2021, 6, 24765−24776